IJAME

Int. J. of Applied Mechanics and Engineering, 2026, vol.31, No.2, pp.88-109
DOI: 10.59441/ijame/218524

NATURAL CONVECTION OF A CASSON-TYPE NANOREFRIGERANT ALONG A VERTICAL PLATE EMBEDDED IN A DISPERSIVE POROUS MEDIUM

H. Nada[1], A.M. Bouaziz[1] and N.M. Bouaziz[2*]
[1]Biomaterials and Transport Phenomena Laboratory, Faculty of Technology, Univ Médea, ALGERIA
[2]Biomaterials and Transport Phenomena Laboratory, Mechanical Engineering, ALGERIA
E-mail: mn_bouaziz@email.com

To address the use of nanorefrigerants of recognized environmental interest, this research focuses primarily on the impacts of thermal dispersion and inertia effect of porous medium. Combined with nanoparticles in natural convection of Casson base nanofluid flow on an embedded vertical plate, heat transfer is then examined. Using technical similarity, the ordinary differential equations resulting from the transformation of the partial differential equations are solved by the III Lobatto discretization of finite differences method through bvp4c @Matlab. The present numerical results are compared with previously obtained similar solutions and they are in good agreement. The significant influences of nanoparticles, thermal dispersion, shape factor, inertial effects of the porous medium, Casson and Eckert parameters on the natural convection flow are highlighted. Maximum values of the Nusselt number are obtained for a high values of γ, R_{ad}, F_0 and low values of the Brownian and thermophoretic diffusions of the nanorefrigerant. Dispersion should not be neglected because of its close connection with the nonlinearity effects induced by the structure of the porous medium. Working with strong inertials effects and permeability of porous medium is more attractive.The novelty of this paper is the extended coupling of diverse phenomena combinations with taking into account the thermal dispersion. Advanced cooling systems in microelectronics, compact heat exchangers, refrigeration and solar collectors are promising for applying the present findings.

Key words: nanorefrigerant, Casson, porous media, dispersion, natural convection

1. Introduction

The addition of low concentration nanoparticles dispersed in a conventional base fluid called nanofluids have emerged for various applications and in wide fields due to their enhanced thermal conductivity. In particular, heat transfer intensification is sought in many systems where rapid heat dissipation rates are critical for trouble-free operation.

In the fields of refrigeration and air conditioning, nanorefrigerants make heat transfer more efficient than conventional refrigerants [1-3]. For example, the thermal conductivity of Al2O3/R1234yf and CuO/R1234yf nano-refrigerants become enhanced with a volume concentration of nano-sized particles by *41.2%* and *148.1%* respectively at *5%* volume concentration, as investigated by Bibin *et al.* [4]. In a review dedicated to nanorefrigerants, Said *et al.* [5] conclude that the concentration of nanoparticles has a considerable impact in improving thermophysical properties and heat transfer efficiency. In their evaluation, Venkataiah and Sthithapragna [6] deduce that nanorefrigerants evolve as one of the promising efficient heat transfer fluids in various thermal engineering applications. They are used in various cooling systems, such as heat exchangers, electronic cooling systems, even in the automotive and aerospace industries. For extended example, they are used in solar thermal collectors to increase heat capture. Recent advanced techniques include preserving cells and organs through cryogenic cooling of biological tissues, and controlling temperature in hyperthermic therapy. In thermal energy storage, nanorefrigerants are well-suited for phase-change materials. They can also

* To whom correspondence should be addressed

increasingly replace classic refrigerants in heat exchangers such as condensers, evaporators, and porous adsorption systems. For strong compatibility, these nanoparticles and refrigerants Al2O3-R134a, CuO-R600a, and TiO2-NH3 are suitable with the aforementioned components. Heat transfer, efficiency, and energy consumption reduction are potentially better compared to nanoparticle-free refrigerant. Experimental work has shown that the incorporation of nanoparticles into a host refrigerant can significantly improve its thermal conductivity, [7-9]. In a horizontal tube, compared to R600a, nano refrigerant HC-R600a has better heat transfer efficiency with condensation flow, Ahmadpour and Akhavan-Behabadi [10].

Adding nanoparticles to a base fluid can significantly alter its rheological behavior, which is particularly relevant for nanorefrigerants. Experimentalwork conducted by Eshgarf and Afrand [11] showed that nanocoolant samples composed of COOH–SiO_2/EG–water functionalized MWCNTs exhibit pseudoplastic rheological behavior despite the base fluid exhibiting Newtonian behavior. The influence of the shape of nanoparticles as well as the shear rate on the rheological behavior of nanofluids is highlighted by Sharma *et al.* [12]. In their review and among other conditions, a great concentration of nanoparticles with high shear rates of the fluid lead to consider a non-Newtonian behavior. Then, if a need for transfer rate regulation arises, the nanoparticles in the nanocoolant raise the yield stress necessary to begin fluid flow. Therefore, a Casson rheology fluid containing nanoparticles with higher viscosity at low strain rates until the yield stress is exceeded may be a suitable behavioral model. In addition to viscoelasticity, the long-term rheological stability of nanorefrigerants under varying temperature and pressure conditions show that the Casson model is appropriate for the complex flow. In experimental investigation, the rheological behaviors of Al2O3/R141b nanorefrigerant is found shear thickening fluid with low shear rates, Mahbubul *et al.* [13]. The Casson fluid effect is investigated in presence of MHD (Magnetohydrodynamic) by Raju *et al.* [14] on natural convection past a vertical plate, on free convection over oscillating vertical plate, Reddy *et al.* [15], and on free convection over an oscillating permeable plate with Soret effect, Prameela *et al.* [16]. In the present time, Srividya *et al.* [17] examined a Casson-nanofluid behavior in an isothermal stretching sheet, while Shamshuddin *et al.* [18] presented an analysis of Casson-ternary nanofluid on stretchy surface. Salawu *et al.* [19] studied a biconvective Casson-nanofluid in rotary disk.

The emerging interest of nanofluids circulating in porous media is furthermore attractive, reducing energy consumption and environmental impact. For nanofluids in porous media, a comprehensive literature review on different studies has presented by Kasaeian *et al.* [20]. Some studies including non-Newtonian nanofluid are cited. Khanafer and Vafai provides a critical review on the applications of nanofluids in porous media [21], while numerical and experimental studies are reported by Menni *et al.* [22]. More recently, the addition of porous materials, nanomaterials and porous fins improve significantly the heat transfer, as noted by Khalaf *et al.* [23]. Similarly, the combination of a refrigerant/nanorefrigerant with a porous medium is also beneficial. Indeed, if the nanoparticles increase the thermal conductivity of the refrigerant/nanorefrigerant, the heat exchange by conduction and convection is greatly improved due to the specific surface area of the porous medium. Usually, the flow through a porous medium is described by different laws, but in the presence of dominant inertial effects, the Darcy-Forchheimer law is the most used. This applies to non-Newtonian nanofluids present with a relatively high velocity in the heterogenous porous medium. Many research studies have been presented involving the Casson nanofluids flow in porous medium. Among others, Nandeppanavar *et al.* [24], Abo-Dahab *et al.* [25], and Sharanayya *et al.* [26] have focused their studies for specific fluids. The rheological interest of the Casson model continuously arouses studies. More recently, Manthramurthy and Vempati [27], with MHD effect by Kumar *et al.* [28], Hafez and Abd-Alla [29] Govindaraj *et al.* [30] have made some new progress in the convective transport of Casson nanofluid in porous medium. The Casson fluid into a porous medium effect is also investigated in presence of MHD by Manideep *et al.* [31] on free convection over an inclined vertical plate, and with non-Darcy porous medium over an inclined surface, Kumar *et al.* [32]. Across a bi-directional Riga sensor device, Panda *et al.* [33] investigate a Casson-hybrid nanofluid in a non-Darcy porous medium.

Hydrodynamic dispersion is often present during nanocoolant flow, due to the difference in pore size. When crossing these connected or unconnected pores the velocities change, resulting in a complex and non-uniform flow. As a result, this generates thermal dispersion responsible for improving heat transfer, as supported by Chandrasekar *et al.* [34]. In addition to molecular thermal diffusion, there is significant

mechanical dispersion in heat and fluid flow for fluid-saturated in porous medium, due to hydrodynamic mixing of liquid particles passing through pores, [35-36]. Thermal diffusion has been explored in a general form by several authors, for example by Fried and Combarnous [37]. Kvernvold and Tyvand [38] studied theoretically the influence of hydrodynamic dispersion on thermal convection in porous media. Later, Hsu and Cheng [39] derived the thermal dispersion conductivity tensor for convection in a porous medium, based on volume averaging method of the velocity and temperature deviations in the pores. Since dispersion was found to be significant at high Rayleigh numbers, Lai and Kulacki [40] reexamined their previous results by including thermal dispersion effects. For a heated vertical plate immersed in a non-Darcean porous medium, a comparison between experimental and theoretical heat transfer rates has been done by Cheng *et al.* [41] and by Plumb and Huenefeld [42]. Based on this comparison Cheng [43] attribute the differences on the ignored dispersion. As a result, the new model developed by the last author led to better agreements with the experimental data. This author 'model is based on the longitudinal and transverse dispersive thermal diffusivities in relation to the velocities. Hong and Tien [44] admit a linear expression of this diffusivity with the velocity. In addition, a proportionality is also included according to the average pore diameter. Thus, thermal dispersion can be modeled through velocity and pore diameter, confirmed experimentally. The effective thermal diffusivity is then as the sum of the molecular diffusivity and the dispersion diffusivity. Reported experimental studies on the determination of effective thermal conductivity are summarized and compared by Özgümüş *et al.* [45]. It should be boted that nonlinear effects characterizing the microscopic inertia and causing thermal dispersion are found to account for 50% of all these effects, as reported by Ait Saada *et al.* [46].

The literature review of works devoted to natural convection of nanofluids - Casson type flowing in a porous medium does not incorporate thermal dispersion despite its importance. This additional thermal transfer is due to flow irregularities in the pores which exists in almost all porous media. Thus, a Casson nanorefrigerant flow in a porous medium under natural convection taking into account the thermal dispersion is studied. Compared to what has been presented in the literature, the novelty of this study combines several phenomena with the use of a dispersive porous medium and highlights the coupled effects. The objective of the analysis is to quantify the variations in dissipated heat transfer following the extended coupling of phenomena. The motivations for the study are multiple, and we aim to numerically determine:

- First, the impact of the rheology of the nanocooler on a vertical plate.
- Second, the impact of thermal dispersion, inertial effects, structural and shape factor of the porous medium on the momentum, heat and fraction of nanoparticles profiles.
- Third, it is also useful to question us about the benefits of adding nanoparticles through thermophoresis and Brownian motion, in this complex case.
- Finally, to show the sensitivity of the parameters involved in the engineering quantities.

2. Analysis

2.1. Problem description and asumptions

Considering a hot wall at constant temperature T_f supplied a continuous heat flux towards the natural convection flow of an adjacent nanorefrigerant, is portrayed in Fig.1. Dissipation takes place in a dispersive porous medium filled with a Casson nanorefrigerant. These assumptions are assumed in this analysis:

- The density in the buoyancy term is dependent-temperature, while others physical properties are assumed to be constant.
- The nanorefrigerant flow obeys to Darcy or Darcy-Forchheimer laws in the porous medium.
- At the hot wall the nanoparticle volume fraction ϕ_w is hypothetically constant.
- Laminar flow occurs in the dynamic boundary layer.
- Local termal equilibrium between the convective nanofluid and the solid part of porous media is assumed everwhere, due to laminar flow in small pores.
- A natural convection and steady-state flow are considered.
- The Boussinesq approximation is adopted to the buonyancy term.

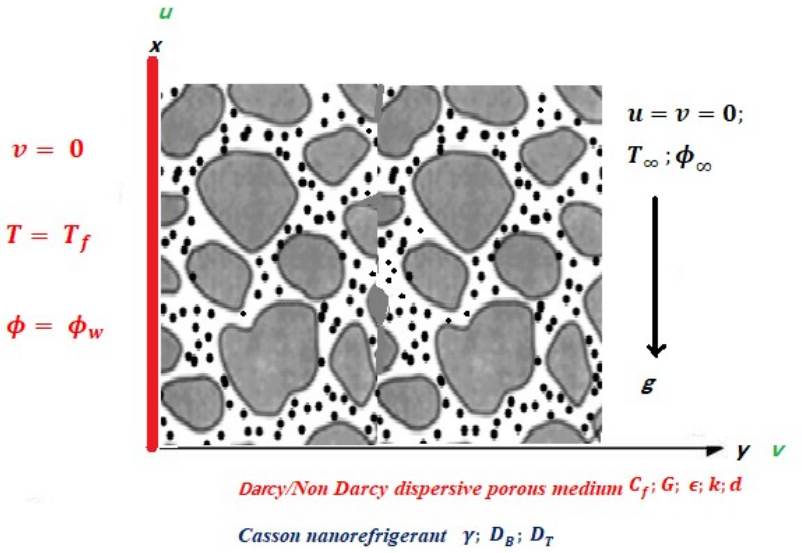

Fig.1. Schematic of physical problem with geometric configuration.

2.2. Casson rheological model

For an isotropic and incompressible flow of Casson nanorefrigerant, the rheological equations known as biviscosity model, is in mathematical form [47-48]:

$$\tau_{ij} = \begin{cases} 2\left(\mu_B + \dfrac{P_y}{\sqrt{2\pi^*}}\right)e_{ij} & \pi^* > \pi^*_c, \\ 2\left(\mu_B + \dfrac{P_y}{\sqrt{2\pi^*_c}}\right)e_{ij} & \pi^* < \pi^*_c \end{cases} \tag{2.1}$$

where $\tau_{ij} = \tau_{xy}$ in 2D flow is the shear stress in the (i,j) element of the deformation rate.

Here $\pi^* = e_{ij}e_{ij}$ with $e_{ij} = e_{xy} = \dfrac{1}{2}\left(\dfrac{\partial v_i}{\partial x_j} + \dfrac{\partial v_j}{\partial x_i}\right)$ becomes here $e_{xy} = \dfrac{1}{2}\left(\dfrac{\partial u}{\partial y} + \dfrac{\partial v}{\partial x}\right) \cong \dfrac{1}{2}\dfrac{\partial u}{\partial y}$.

μ_B is the plastic dynamic viscosity of the present fluid and P_y refers to the yield stress of the fluid. The critical value of the deformation rate is π^*_c. u and v are the velocities.

For the case $\pi^* > \pi^*_c$, and above considerations, Eq.(2.1), leads to:

$$\tau_{ij} = \tau = \left(\mu_B + \frac{P_y}{\sqrt{2\pi^*}}\right)\frac{\partial u}{\partial y}. \tag{2.2}$$

Introducing γ a constant Casson fluid parameter as $\gamma = \dfrac{\sqrt{2\pi^*}\,\mu_B}{P_y}$, then, it is well to deduce the yield stress and the dynamic equivalent viscosity μ so that,

$$\tau=\mu_B\left(1+\frac{1}{\gamma}\right)\frac{\partial u}{\partial y} \quad \text{and} \quad \mu=\left(\mu_B+\frac{P_y}{\sqrt{2\pi^*}}\right)=\mu_B\left(1+\frac{1}{\gamma}\right). \tag{2.3}$$

This result is also applicable to viscous dissipation terms.

2.3. Mathematical model of the problem

For the present problem, the governing of boundary layers equations, written according to the above assumptions, are as follows:

$$\frac{\partial u}{\partial x}+\frac{\partial u}{\partial y}=0, \tag{2.4}$$

$$\frac{\partial p}{\partial x}=-\left(1+\frac{1}{\gamma}\right)\frac{\mu}{k}u-\rho_{f\infty}\frac{C_f}{\sqrt{k}}u^2+\left(1+\frac{1}{\gamma}\right)\mu\frac{\partial^2 u}{\partial y^2}+(1-\phi)\rho_{f\infty}g\beta_T\left(T-T_\infty\right)+ \\ -\left(\rho_p-\rho_\infty\right)g\left(\phi-\phi_\infty\right), \tag{2.5}$$

$$\frac{\partial p}{\partial y}=0, \tag{2.6}$$

$$u\frac{\partial T}{\partial x}+v\frac{\partial T}{\partial y}=\frac{\partial}{\partial y}\left[\left(\alpha_m+Gdu\right)\frac{\partial T}{\partial y}\right]+\frac{\nu}{C_p}\left(1+\frac{1}{\gamma}\right)\left(\frac{\partial u}{\partial y}\right)^2+\left(1+\frac{1}{\gamma}\right)\frac{\nu u^2}{kC_p}+ \\ +\frac{C_f u^3}{C_p\sqrt{k}}+\frac{\varepsilon(\rho c)_p}{(\rho c)_f}\left[D_B\frac{\partial\phi}{\partial y}\frac{\partial T}{\partial y}+\frac{D_T}{T_\infty}\left(\frac{\partial T}{\partial y}\right)^2\right], \tag{2.7}$$

$$u\frac{\partial\phi}{\partial x}+v\frac{\partial\phi}{\partial y}=\varepsilon\left(D_B\frac{\partial^2\phi}{\partial y^2}+\left(\frac{D_T}{T_\infty}\right)\frac{\partial^2 T}{\partial y^2}\right). \tag{2.8}$$

In this mathematical formulation, a linear expression for thermal diffusivity due to hydrodynamic dispersion is adopted, in addition to molecular diffusion, as stated by Hong and Tien [44].

The cross-derivation of Eqs (2.5-2.6) with respect to the y and x coordinates respectively, leads to a single equation of motion of the nanofluid.

$$\frac{\partial}{\partial y}\left[\left(1+\frac{1}{\gamma}\right)u+\frac{C_f\sqrt{k}}{\nu}u^2\right]=(1-\phi_\infty)\rho_{f\infty}\frac{k}{\mu}g\left(\beta_T\frac{\partial T}{\partial y}\right)-\left(\rho_p-\rho_\infty\right)\frac{g}{\mu}k\frac{\partial\phi}{\partial y}. \tag{2.9}$$

The boundary conditions for the natural convection problem under investigation were set as for:

$$y=0, \quad v=0, \quad T=T_f, \quad \phi=\phi_w, \tag{2.10}$$

and if

$$y\to\infty: u=v=0, \quad T\to T_\infty, \quad \phi\to\phi_\infty. \tag{2.11}$$

Introducing the following variables:

$$\eta = \frac{y}{x} Ra_x^{\frac{1}{2}}, \quad f(\eta) = \frac{\psi}{\alpha_m Ra_x^{\frac{1}{2}}}, \quad \left(u = \frac{\partial \psi}{\partial y} \quad \text{and} \quad v = -\frac{\partial \psi}{\partial x} \right),$$
$$\theta = \frac{T - T_\infty}{T_f - T_\infty}, \quad s = \frac{\phi - \phi_\infty}{\phi_w - \phi_\infty}, \tag{2.12}$$

where

$$Ra_x = \frac{(1 - \phi_\infty)\rho_{f\infty} \beta_T (T - T_\infty) gkx}{\mu \alpha_m}. \tag{2.13}$$

Using these new variables, the governing equations, Eqs (2.7–2.11) reduces to a self similar system ODE (ordinary differential equations) and becomes a BVP (boundary value problem).

$$f'' \left(\left(1 + \frac{1}{\gamma} \right) + 2F_0 Ra_d f' \right) = \theta' - N_r s', \tag{2.14}$$

$$\theta'' \left(1 + GRa_d f' \right) = -\frac{1}{2} f\theta' - GRa_d \theta' f'' - \frac{E_C}{P_r} \left(1 + \frac{1}{\gamma} \right) Ra_d^2 (f'')^2 - \frac{E_c S Ra_d}{P_r} (f')^2 +$$
$$- \frac{E_c S Ra_d}{P_r} F_0 (f')^3 - N_b s'\theta' - N_t (\theta')^2, \tag{2.15}$$

$$s'' = -\frac{1}{2} L_n f s' - \frac{N_t}{N_b} \theta'', \tag{2.16}$$

$$\eta = 0 : f = 0°, \quad \theta = 1, \quad \text{and} \quad s = 1, \tag{2.17}$$

$$\eta \to \infty : f' = 0, \quad \theta \to 0, \quad \text{and} \quad s \to 0. \tag{2.18}$$

In the transformation, the dimensionless numbers in Eqs (2.14)-(2.16) are defined as follow:

$$F_0 = \frac{c_{f\sqrt{k}}}{\vartheta d} \alpha_m, \quad N_r = \frac{(\rho_p - \rho_\infty)(\phi_w - \phi_\infty)}{(1 - \phi_\infty)\rho_{f\infty} \beta_T (T_f - T_\infty)}, \quad N_b = \frac{\varepsilon (\rho c)_p D_B (\phi_w - \phi_\infty)}{(\rho c)_f \alpha_m},$$
$$P_r = \frac{\vartheta}{\alpha_m}, \quad S = \frac{d^2}{k}, \quad N_t = \frac{\varepsilon (\rho c)_p D_T (T_f - T_\infty)}{((\rho c)_f \alpha_m)}, \quad E_c = \frac{\vartheta^2}{C_p (T_f - T_\infty) d^2}, \tag{2.19}$$
$$L_n = \frac{\alpha_m}{\varepsilon D_B}, \quad Ra_d = \frac{(1 - \phi_\infty)\rho_{f\infty} \beta_T (T_f - T_\infty) gkd}{\mu \alpha_m}.$$

The meaning of all the symbols are reported in the nomenclature. The most quantitative engineering parameter of interest in this context is the Nusselt number. The ratio between the convective heat in the nanorefrigerant and the conductive heat in the solid plate is represented by this dimensionless number. Equalizing these two heat transfers following their respective laws:

$$q_w = \left[-\lambda \left(\frac{\partial T}{\partial y} \right) \right]_{y=0} = h\left(T_w - T_\infty \right) \tag{2.20}$$

and using the above scaling transformation, the physical interest quantity is in dimensionless form:

$$Nu_x Ra_x^{-\frac{1}{2}} = -\left[1 + GRa_d f'(0) \right] \theta'(0). \tag{2.21}$$

3. Results and discussion

3.1. Methodology

Applied the similarity transformation, the obtained ordinary differential Eqs (2.14-2.18) are strongly coupled and nonlinear. The Lobatto IIIa discretisation formulas, belongs to implicit Runge-Kutta methods, is suitable for increasing accuracy. For its implementation on bvp4c of @Matlab, the global interval is first divided into smaller mesh-intervals. Then, an approximate solution at certain so-called collocation points or Lobatto points is initiated by cubic polynomials using the Newton's method. These polynomial functions should matched the values found at all these points. At the current process, the mesh is adaptively refined to improve accuracy according to the residual between the derivative and the corresponding values predicted by the polynomials. This ensures higher stability and continuity of the solution for first derivative and the accuracy near boundaries. The method is second-order accurate globally and converges quadratically. The tolerance of 10^{-6} is accepted as a convergence criterion to respect the boundary conditions helped by providing a good initial guess.

After some trials in the η-direction, a larger number of η_{max} are selected until the calculated functions matched the prescribed boundary condition. It found that $\eta_{max} = 7 - 10$.

3.2. Code validation

A further step consisted of running the developed code by adjusting it for a classical fluid without nanoparticles with Newtonian fluid/nanofluid flow in a porous Darcy medium ($F_0 = 0$) and without dispersion ($G = 0$). In addition, dissipations, other than viscous, were ignored in this validation task.

Table 1. Comparison of the results and those in [49] and [50] for $-\theta'(0)$.

Conditions		*-θ'(0)*		
		In [49]	In [50]	Present results
Case 1	Mono diffusive regular fluid $Nc = Nr = Nb = Nt = 0$; $Ln = 10$	*0.4439*	*0.44377568*	*0.442873*
Case 2	Mono diffusive nanofluid $Nc = 0$; $Nr = Nb = Nt = 0.2$; $Ln = 10$	*0.3344*	*0.33417924*	*0.333256*

The following Tab.1. presents a relevant comparison for two cases to check the accuracy of the code used. The same conditions are similar with those of Nield and Kusnetsov [49] and Hanini and Bouaziz [50] when putting $\gamma = 1000$, $G = 0$, $F_0 = 0$, $Ec = 0$, $Ln = 10$ and active nanoparticles $s = 1$ at $\eta = 0$.

Table 1 shows that the computational code is error-free.

3.3. Numerical results

Comprehensive solutions have been obtained and are presented through Figs 2-8. Numerical calculations were performed to establish velocity f', temperature θ, and nanoparticle volume fraction ϕ profiles in the boundary layers. This is to quantify the influence of parameters describing flow characteristics on these profiles. The relevant different values were chosen to highlight the effects of inertial parameter of porous medium F_0, Casson parameter γ, Eckert number Ec, dispersion coefficient G, shape factor of porous medium S, Brownian diffusion and thermophoretic diffusion parameters Nb and Nt, All results are presented in graphs involving variations of Rayleigh number Ra_d.

In these calculations, The thermal dispersion coefficient G measures the degree of thermal dispersion in the porous medium. Its range varies from *0.01-10* varying between a dominant conduction and very rare dispersions encountered. Here, $G = 0, 0.3, 0.6$ as an illustration showing the case of non-dispersion of the porous medium and the realistic cases of thermal dispersion. For the intensity of natural convection Ra_d, the values *0.5*; *2* et *3* correspond to a choice compatible with the porous medium. F_0 is naturally zero for flow obeying Darcy's law. A single value of *0.5* is considered for the case where Forsheimer's law is applicable. In abnormal porous media, this coefficient can be equal to the limit value $F_0 = 10$, in relation to the nature of the materials. For the Casson parameter (γ), the simulation is carried out with three values within the practical limits of viscoelasticity, 10^{-5} for an exceptionally Casson behavior, either *1.5* with a rheologically average of the base nanorefrigerant and $\gamma = 10$ nearer to Newtonian behavior. In the typical ranges (*0.01-100*), the shape factor S is reduced to $[0.1, 5, 10]$ for low to moderate resistance of the porous medium to flow. The range of variations of the Eckert number is between *0.01-1*, but for the present case, it is chosen $[0.1, 0.2, 0.4]$ to highlight its effect. Note that number represents viscous flows relative to thermal storage. The choice of *0.1* and *0.3* both for Nb and Nt indicate a very high intensity of Brownian motion and nanoparticles which are often in relation to the concentration. In the present computations, the following parameters are prescribed: $L_n = 10$, $Pr = 1$, and $N_r = 0.2$ corresponding to low coupling between the thermal and nanoparticles effects.

For a Darcéen porous medium, one can observe that the thickness of the boundary layer is greater than in a non-Darcéen porous medium. The development of the boundary layer is slow, characterized by a more abrupt profile in Darcy flow case. Due to sliding at the wall-nanocooler interface, the velocity profile is more uniform in the second case, following a reduction in the wall velocity, Fig.2(a).

a)

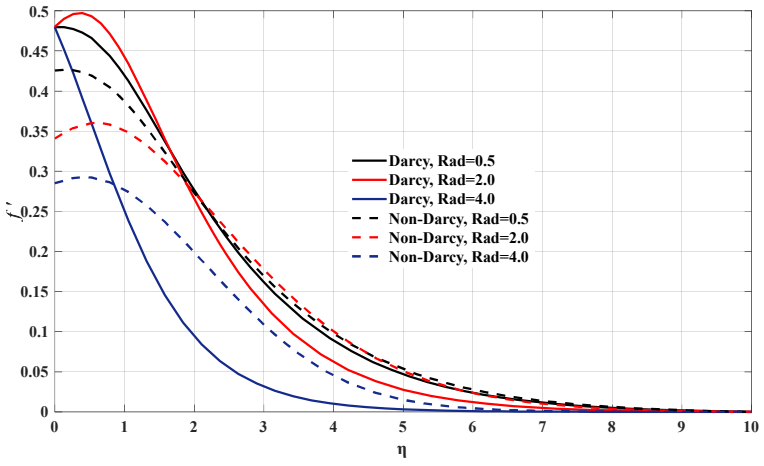

Fig.2. The influence of structural and thermo-physical parameter of porous medium F_0 on f', θ and profiles ($F_0 = 0$ Darcy flow; $F_0 = 0.5$ non Darcy flow example).

b)

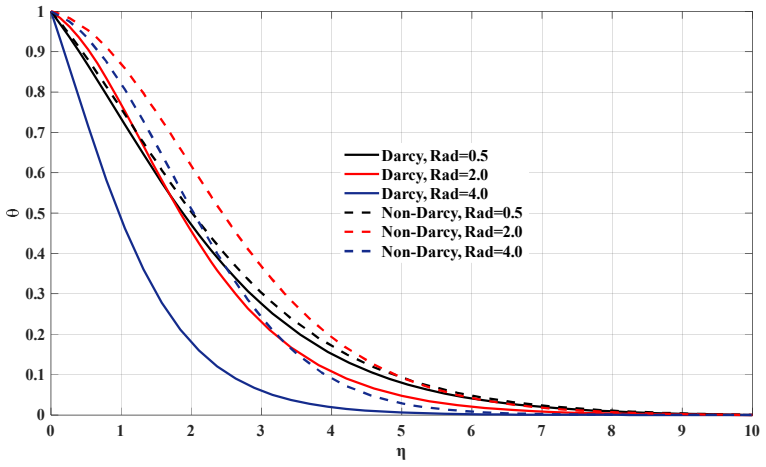

c)

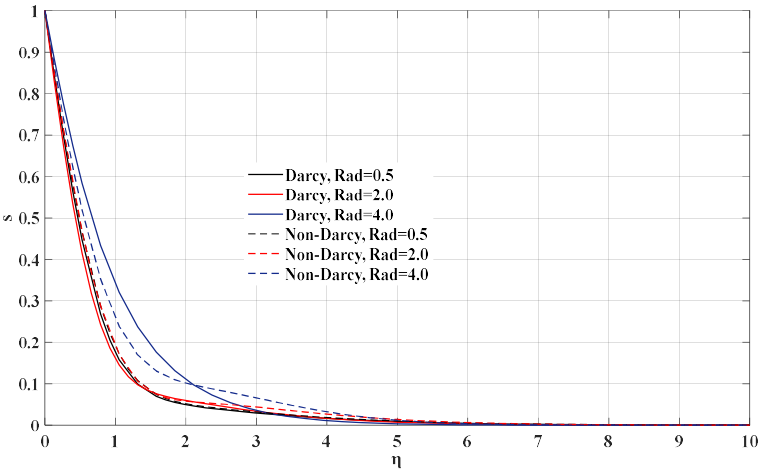

Fig.2. cont. The influence of structural and thermo-physical parameter of porous medium F_0 on f', θ and profiles ($F_0 = 0$ Darcy flow; $F_0 = 0.5$ non Darcy flow example).

This is explained by a typical development dependent on significant inertial effects. The effect of the strong natural convection is extincted for a Darcéen porous medium, on the other hand it is more uniform in the other case. Due to a high permeability of the porous medium, the increasing influence of inertia favors convection and a difference is observed compared to the Darcéen medium. Fig.2(b) shows regular and quasi-linear temperature profiles for the Darcean porous medium. The temperature is higher in the non-Darcean porous medium due to strong inertial effects and consequently leads to efficient and rapid thermal transport. It can be noted in Fig.2(c) that the gradients of the volume fraction of nanoparticles are almost the same in the regions near the wall, but tend to separate as Ra_d increases. The greater diffusion of nanoparticles driven by the inertial effect of the base fluid is evident.

The dimensionless velocity and temperature profiles of the boundary layer for different Casson parameters are shown in Figs 3(a) and 3(b). It is clear that low values of the Casson parameter, expressing very viscous Newtonian rheology, result in decrease in velocity to zero, Fig.3(a). On the contrary, and as the base fluid is naturally more following Casson behavior, resistances to flow decrease and great and reduced by half near the wall velocities will be observed. In other words, the nanofluid becomes more free to flow. In all cases, the effect of Casson rheology is predominant compared to the effect of natural convection. The temperature in relation to the Casson parameter, Fig.3(b), shows a great slope to profiles with γ.

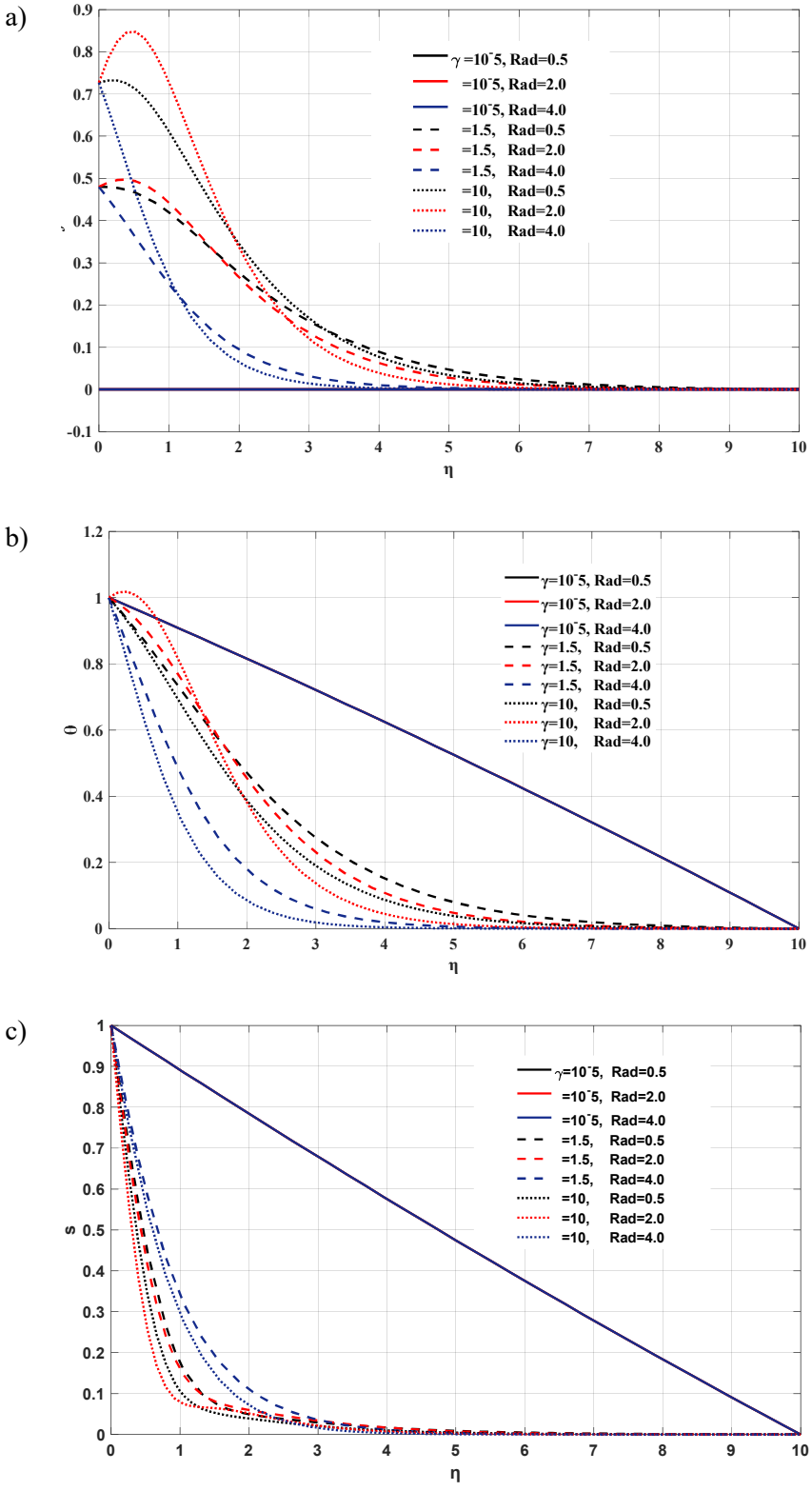

Fig.3. The influence of Casson parameter γ on f', θ and s profiles.

Thus, the temperature decrease quickly in the boundary layer, explained by a favorable thermal diffusion. The thickness of the thermal boundary layers is reduced if the Casson parameter increases. In Fig.3(c), because γ increases, the transport of nanoparticles is easier. Linear curves are obtained in Figs 3(b) and 3(c) when the nanorefrigerant becomes very highly viscous with effective viscosity due to very small γ. In this case, the temperature and nanoparticle distribution is more uniform due to reduction in both heat conduction and nanoparticle transport attributed to low velocity.

The velocity and temperature profiles are strongly modified in relation to the Eckert number, Figs 4(a) and 4(b). As it can be seen in these figures, sensible influence on the velocity profile is noted with relatively weak Ra_d and this trend is inversed for great values of Ra_d. This can be explained one part by dominant natural convection in front of low thermal dissipation due to viscosity. On other part, more viscous dissipation combined to higher buoyancy force led to the curves corresponding to $Ec = 0.4$. The greatest impacts are noted for high Ra_d and *Ec* translated by the velocities decreasing very rapidly further from the wall. Observing the temperature profile similar to that of the velocities, one can attribute these variations to the competitive effects between the buoyancy force, the thermal dissipation generated due to viscosity and the thermal dispersion in porous medium. A high *Ec* due to the increase in temperature promotes Brownian motion, which results in a more uniform concentration of nanoparticles. However, the effect of *Ec* on fraction volumique is more located near the wall, except when *Ec* is very high, Fig.4(c).

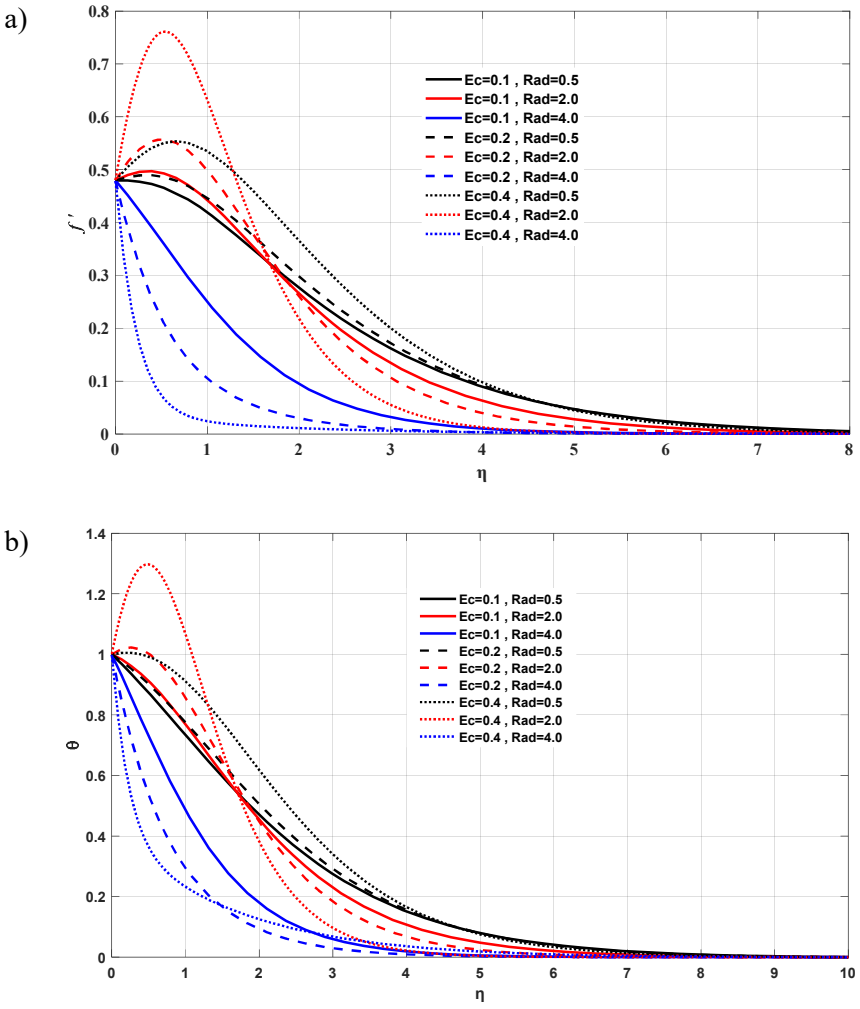

Fig. 4. The influence of Eckert number *Ec* on f', θ and s profiles.

c)

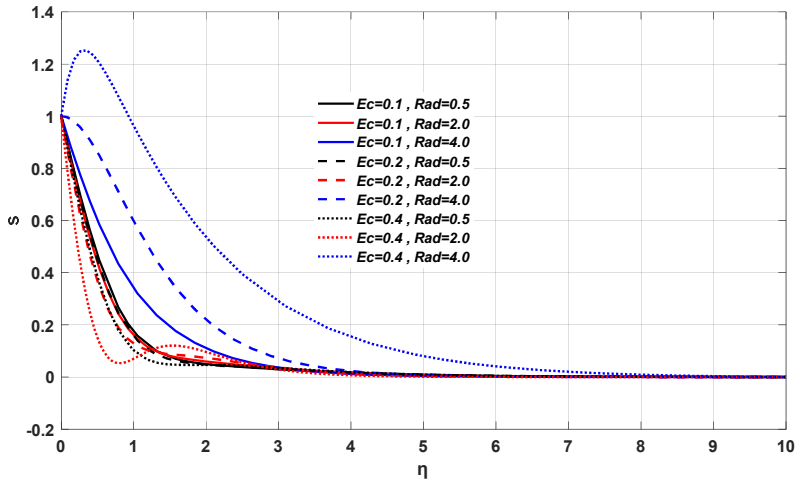

Fig.4 cont. The influence of Eckert number Ec on f', θ and s profiles.

a)

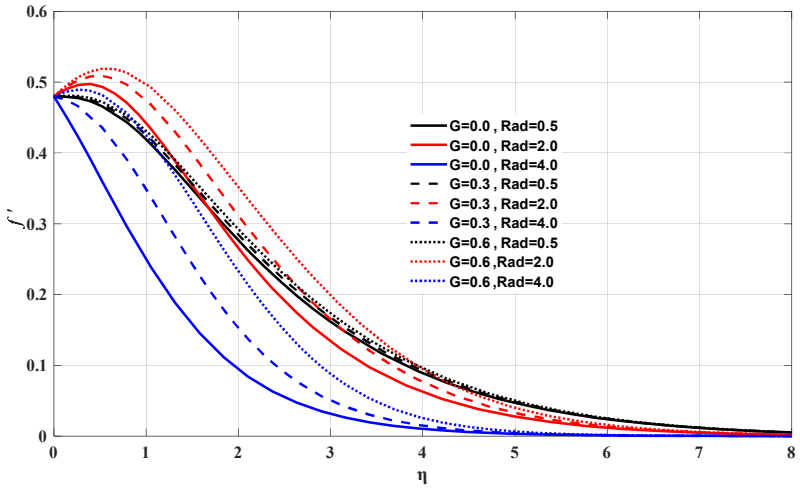

b)

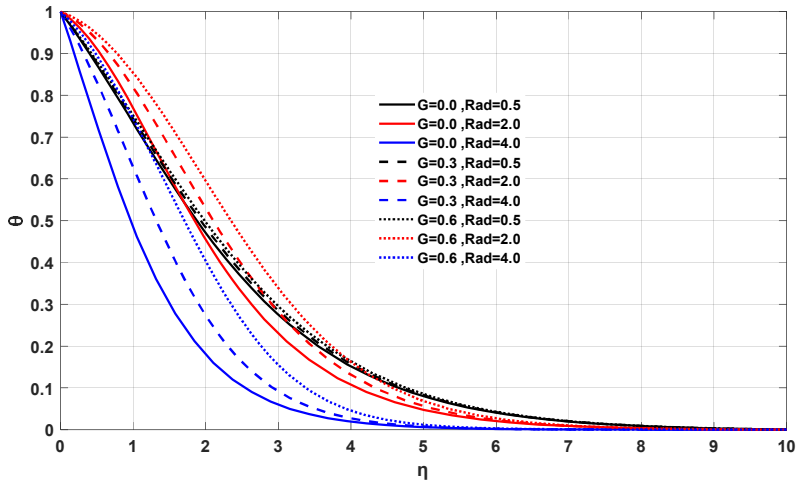

Fig.5. The influence of non dispersive/dispersive parameter porous medium (G) on f', θ and s profiles.

c)

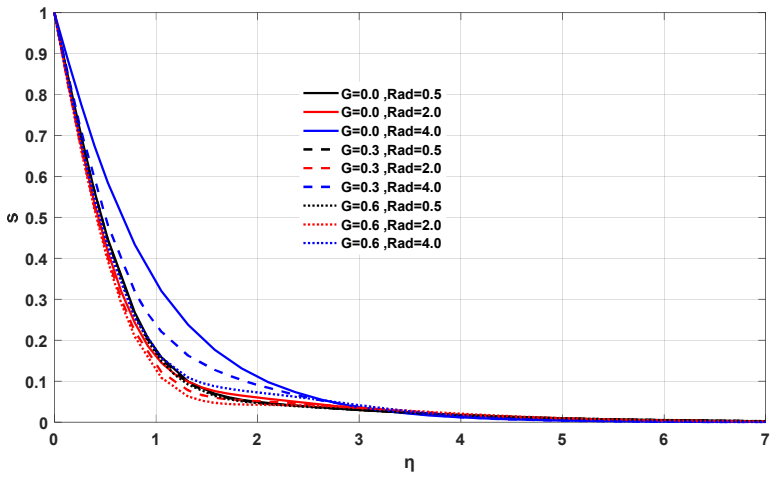

Fig.5 cont. The influence of non dispersive/dispersive parameter porous medium (G) on f', θ and s profiles.

Figure 5(a) is plotted to assess the influence of thermal dispersion on the velocity distribution. It is observed that taking thermal dispersion into account substantially affects the velocity profiles. This effect is naturally more noticeable and becomes non-negligible for strong natural convection. It is also interesting to note that in the latter case the boundary layer thickness is reached more quickly. However, the differences in the curves begin to fade as Ra_d becomes lower. The same trends are found for the temperature profile, with slightly smaller gaps than for the velocities, Fig.5(b). This can be attributed to the diffusion generated by thermal dispersion and which is added to the molecular diffusion. The origin of the dispersion here is mechanical, where there are differences in the trajectory of the nanocooler molecules when they pass through the different pores. Circulating in wide or narrow pores, the speeds vary, leading to dispersion accompanied by thermal dispersion. Thus, it is not correct to neglect this complementary diffusion linked to the porous medium and dependent on its nature and the speed flow. As expected, for the nanoparticle concentration profile, Fig.5(c), the thermal dispersion has no notable impact on the distribution.

The important dimensionless shape factor S refers to a value that is affected by the structural form of the porous medium, especially the average pore diameter rapported to its permeability. In porous media characterized structurally by heterogeneity or anisotropy, flow can be influenced by pore size, shape and pore network connectivity in relation to permeability resulting in greater hydrodynamic dispersion. Therefore, high values of S mean large pore size values relative to low permeabilities.

a)

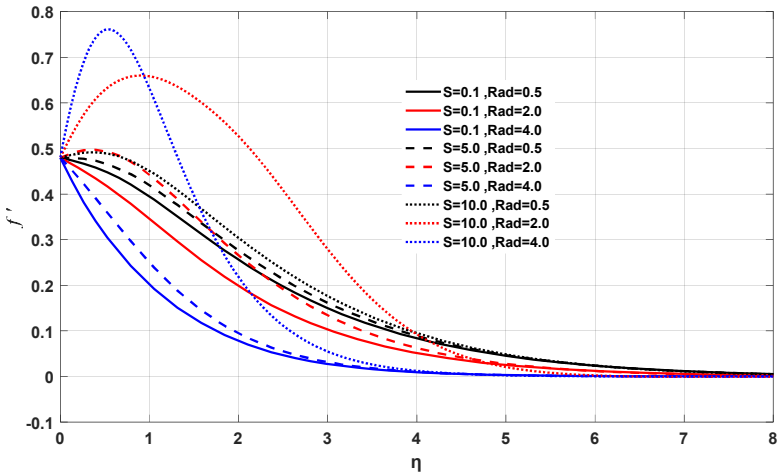

Fig.6. The influence of the shape factor of porous medium S on f', θ and s profiles.

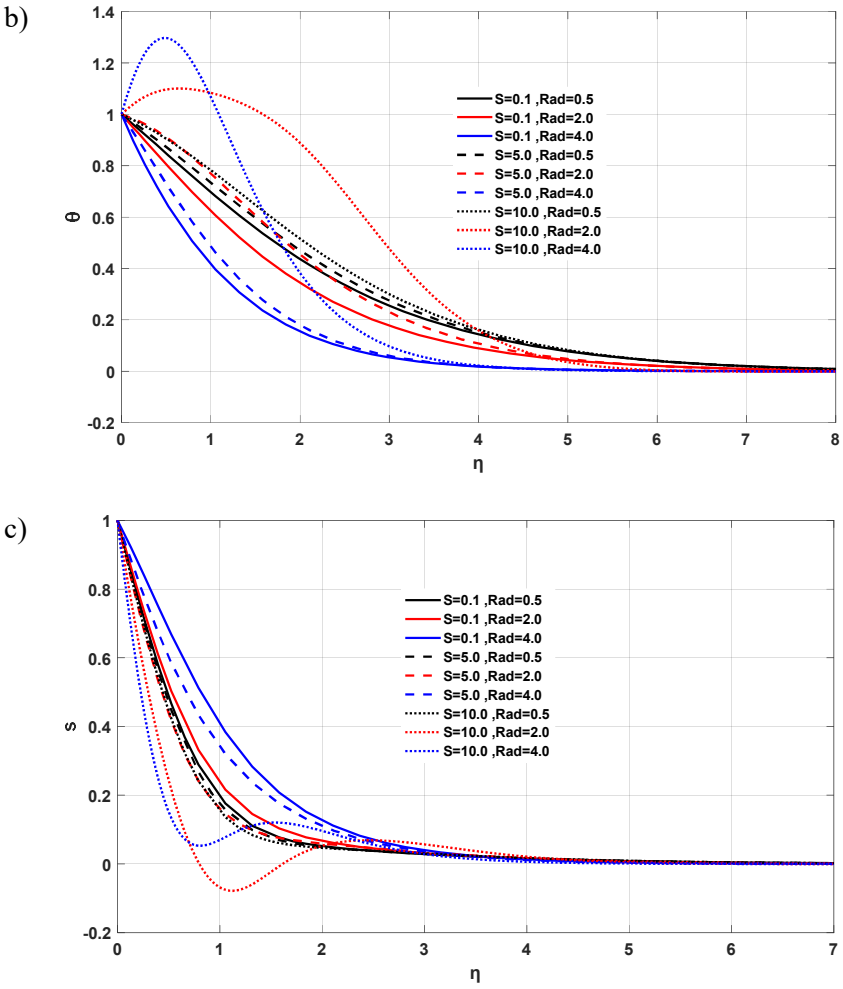

Fig.6. cont. The influence of the shape factor of porous medium S on f', θ and s profiles.

In Figs 6(a)-(b), it is found that if S is high, both velocities and temperatures become more uniform especially for high Ra_d numbers. Since the nanocoolant flows more freely in the porous medium, explains the stability flow and temperature. Figure 6(c) indicates that the concentration of the nanoparticles is slightly promoted near the wall as S and Ra_d increase.

The Brownian random diffusion parameter Nb expresses the intensity of collisions between nanoparticles, transforming kinetic energy into thermal energy. In Figs 7(a)-(b), the increase in Nb affect slightly the velocity profile in accordance with the weak influence on the temperature profile. The distribution of the volume fraction of nanoparticles being unchanged, Fig.7(c), that explains the previous profiles. Noting that at $Ra_d = 0.4$ the variation of s is insufficient to induce an effect on the temperature. It is also understandable that with a high viscosity Casson nanocooler, the other mechanisms involved for the temperature evolution are more important compared to the present phenomenon. Moreover, thermophoresis which consists of a migration of nanoparticles from hot regions to cold regions, in Figs 8(a)-(c), obviously follows the same trend but reversed when Nt varies. Intriguing results (Fig.7) can be explained by the different dependence of viscosity on Nb and Nt (or D_B and D_T).

Table 2 demonstrates the changes in the Nusselt number under the influence of parameters involved in this study, namely G, Ra_d, F_0, γ, S, Pr, Ec, Nr, Nb and Nt. In this table, maximum values of the Nusselt number are obtained for a high values of γ, Ra_d, F_0 and low values of the Brownian and thermophoretic diffusions of the nanorefrigerant.

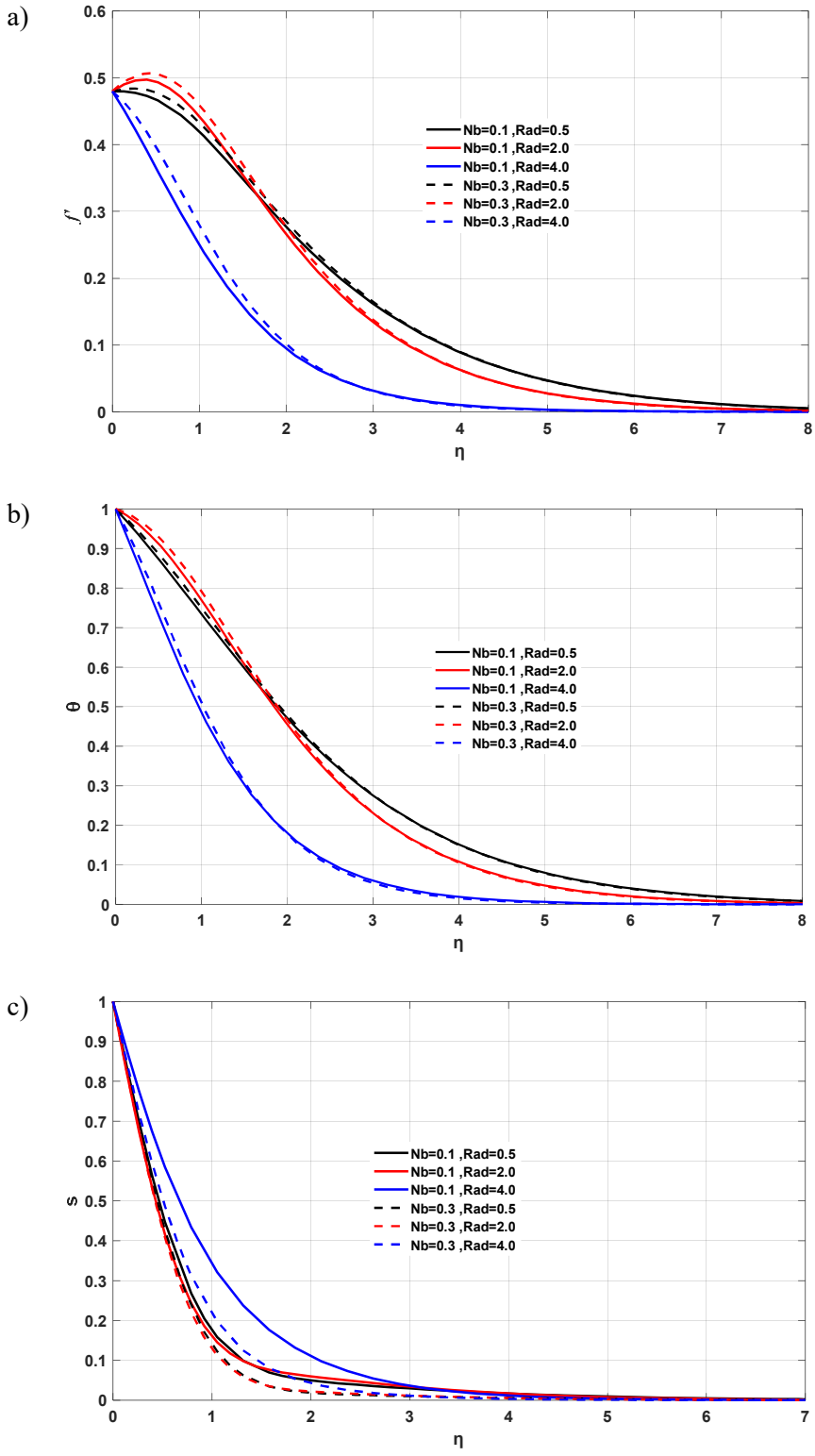

Fig.7. The influence of the Brownian diffusion parameter *Nb* on f', θ and *s* profiles.

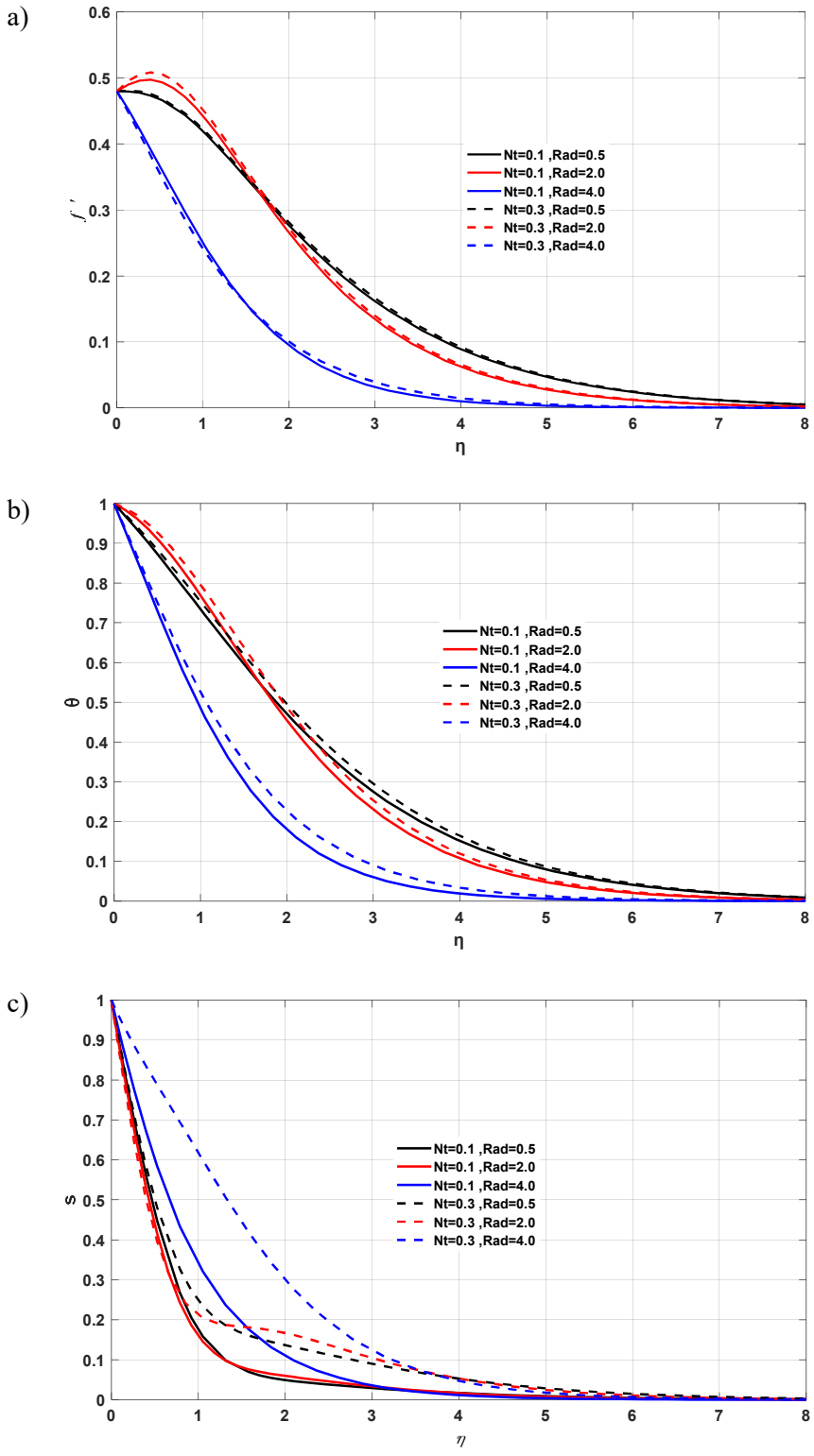

Fig.8. The influence of the thermophoretic diffusion parameter *Nt* on f', θ and *s* profiles.

Table 2. Effect of physical parameters on local Nu_x number.

G	Ra_d	F_0	γ	S	Pr	Ec	Nr	$Nb = Nt$	$f'(0)$	$\theta'(0)$	$Nu_x Ra_x^{-1/2}$
0.2	0.5	0.3	0.7	1	3	0.1	0.1	0.3	0.3624	0.1911	0.1980
0	–	–	–	–	–	–	–	–	0.3624	0.1934	0.1934
0.4	–	–	–	–	–	–	–	–	0.3624	0.1890	0.2027
0.2	0.1	–	–	–	–	–	–	–	0.3688	0.1951	0.1965
–	2	–	–	–	–	–	–	–	0.3417	0.1888	0.2146
–	0.5	0	–	–	–	–	–	–	0.3705	0.1929	0.2000
–	–	0.6	–	–	–	–	–	–	0.3549	0.1895	0.1962
–	–	0.3	15000	–	–	–	–	–	0.8030	0.2768	0.2990
–	–	–	0.1	–	–	–	–	–	0.0803	0.1042	0.1050
–	–	–	0.7	0	–	–	–	–	0.3624	0.1935	0.2005
–	–	–	–	5	–	–	–	–	0.3624	0.1813	0.1872
–	–	–	–	1	0.1	–	–	–	0.3624	0.1519	0.1574
–	–	–	–	–	7	–	–	–	0.3624	0.1919	0.1989
–	–	–	–	–	3	0.2	–	–	0.3624	0.1924	0.1994
–	–	–	–	–	–	0.4	–	–	0.3624	0.1898	0.1967
–	–	–	–	–	–	0.1	–	–	0.4017	0.1948	0.2026
–	–	–	–	–	–	–	0.2	–	0.3229	0.1873	0.1933
–	–	–	–	–	–	–	0.1	0.1	0.3624	0.2411	0.2498
–	–	–	–	–	–	–	–	0.5	0.3624	0.1512	0.1567

Physically, for the first parameter one can explain that the yield stress decreases when γ increases provoking an increase of nanocooler velocity and less temperature in the boundary layer. Working with strong inertials effects and permeability of porous medium is more attractive. These relative variations are also observed with moderate values of *Pr*. Moreover, low values of the local Nusselt number can be attributed to weak γ and *Pr* that expressed a greater heat diffusivity than momentum diffusivity.

4. Conclusions

A mathematical model is developed to study the natural convection of a Casson fluid-based nanocooler flowing in a dispersive porous medium. The insertion of a hot vertical plate diffuses heat to the nanocooler. An ODE system was obtained using the similarity technique by conversion of the partial differential equations. The finite difference method following the Lobatto III discretization was used to solve the converted system. Then, numerical results illustrate the impact of the dimensionless variables involved on the different boundary layer profiles. The noteworthy results of this study are as follows:

- As inertial effects F_0 of porous medium and Ra_d are high, velocities become slow and are greatly reduced near the wall. So, temperature are more uniform and the concentration of the nanoparticles is high near the wall.
- As γ and Ra_d are high, fast velocities are reduced by half near the wall and temperature profile and concentration profile show more great slope.
- As *Ec* and Ra_d are high, the velocity is more rapid, temperature decreases strongly, both are sensitive to great *Ec,* and the concentration of nanoparticles is more located near the wall, except when *Ec* is very high
- As *G* and Ra_d are high, the velocity and temperature decrease, and near the wall the nanoparticles are concentrated.

- As S the shape factor and Ra_d are high, The velocity and temperature are more uniform due to natural convection effect and incresed near the wall where high fraction of nanoparticles remains.
- In the limit of the values attributed to *Nb*, the velocities are affected slightly by their changes, while the temperature is not changed and the nanoparticles reside near the wall. These effects are reversed for *Nt*.
- Maximum values of the Nusselt number are obtained for a high values of γ, Ra_d, F_0 and low values of the Brownian and thermophoretic diffusions of the nanorefrigerant.
- Dispersion should not be neglected because of its close connection with the nonlinearity effects induced by the structure of the porous medium.
- Working with strong inertials effects and permeability of porous medium is more attractive.

Distinguished by the effect of thermal dispersion in a porous medium and the interest in the extended coupling of phenomena, the implications of this study in practical applications such as:

– advanced cooling systems in microelectronics or in compact heat exchangers, refrigeration.
– solar collectors and heat storage devices.
– thermal regulation of pseudoplastic biological fluids, will be improved by the introduction of porous media, taking into account dispersion for dissipative nanorefrigerants/nanofluids. However, the main limiting factors for this study are:
– the effects of sedimentation of undefined nanoparticles
– the exact knowledge of the complexity of the actual pore shape, idealized here.

The optimization of the above mentioned parameters can also be carried out for various nanorefrigerants which may be helpful for a specific design.

Further work is needed to validate the results using an experimental approach, and to explore hybrid nanocoolers or other complex geometries using 3D modeling.

Nomenclature

Cf – Forchheimer coefficient

Cp – specific heat at constant pressure $\left[J/Kg\cdot K\right]$

D_B – brownian diffusion coefficient $\left[m^2/s\right]$

D_T – thermophoretic diffusion coefficient $\left[m^2/s\right]$

d – pore diameter $\left[m\right]$

Ec – Eckert number

F_0 – structural and thermo-physical parameter of porous medium

f – dimensionless stream function

f – wall temperature-index

G – thermal dispersion coefficient

g – gravitational acceleration $\left[m/s^2\right]$

h – heat transfer coefficient $\left[W/m^2\cdot K\right]$

k – permeability of the porous medium $\left[m^2\right]$

Ln – nanorefrigerant Lewis number

Nb – Brownian diffusion parameter

Nr – buoyancy ratio parameter

Nt – thermophoretic diffusion parameter

Nu_x – local Nusselt number

Pr – Prandtl number

p – pressure of nanorefrigerant nanofluid $\left[N/m^2\right]$

p – nanoparticle-index

q_w – heat flux on the wall $\left[W/m^2\right]$

Ra_d – Rayleigh number-pore diameter

Ra_x – local Rayleigh number-x

S – porous media shape factor parameter

s – dimensionless nanoparticle volume fraction

T – temperature $\left[K\right]$

u,v – velocity in x, y directions $\left[m/s\right]$

ν – kinematic viscosity $\left[m^2/s\right]$

x,y – coordinates $\left[m\right]$

α_m – molecular thermal diffusivity of the porous medium $\left[m^2/s\right]$

β_T – volumetric thermal expansion coefficient $\left[1/K\right]$

γ – Casson parameter

ε – porosity

η – pseudo-similarity variable

θ – dimensionless temperature

λ – thermal conductivity of the plate $\left[W/m\cdot K\right]$

μ – dynamic viscosity $\left[N\cdot s/m^2\right]$

$(\rho c)_f$ – heat capacity of the nanorefrigerant $\left[J/m^3\cdot K\right]$

$(\rho c)_p$ – effective heat capacity of the nanoparticule materiel $\left[J/m^3\cdot K\right]$

φ – nanoparticle volume fraction

Ψ – stream function $\left[m^2/s\right]$

∞ – out the boundary layer-index

References

[1] Kasaeian A., Hosseini S.M., Sheikhpour M., Mahian O., Yan W.M. and Wongwises S. (2018): *Applications of eco-friendly refrigerants and nanorefrigerants: A review*.– Renew. Sustain. Energy Rev., vol.96, pp.91-99. https://doi.org/10.1016/j.rser.2018.07.033.

[2] Tashtoush B.M., Moh'd A A.N. and Khasawneh M.A. (2017): *Investigation of the use of nano-refrigerants to enhance the performance of an ejector refrigeration system*.– Appl. Energy, vol.206, pp.1446-1463. https://doi.org/10.1016/j.apenergy.2017.09.117.

[3] Subramani N. and Prakash M.J. (2011): *Experimental studies on a vapour compression system using nanorefrigerants*.– Int. J. Eng. Sci. Tech., vol.3, No.9, pp.95-102. DOI:10.4314/ijest.v3i9.8.

[4] Bibin B.S., Bhramara P., Mystkowski A. and Gundabattini E. (2024): *Predictive analysis on the influence of AL2O3 and CuO nanoparticles on the thermal conductivity of R1234yf-based refrigerants*.– Acta Mech. Autom., vol.18, No.3, pp.474-482. DOI:10.2478/ama-2024-0050.

[5] Said Z., Rahman S.M.A., Soheil M.A., Bahman A.M., Alim M.A., Shaik S., Radwan A.M. and El-Sharkawy I. (2023): *Nano-refrigerants and nano-lubricants in refrigeration: Synthesis, mechanisms, applications, and challenges*.– Appl. Therm. Eng., vol.233, 121211. https://doi.org/10.1016/j.applthermaleng.2023.121211.

[6] Venkataiah S. and Sthithapragna G. (2023): *Comprehensive evaluation of nano refrigerants: A review*.– Mater. Today, vol.72, pp.937-942. https://doi.org/10.1016/j.matpr.2022.09.094.

[7] Jiang W., Ding G. and Peng H. (2009): *Measurement and model on thermal conductivities of carbon nanotube nanorefrigerants*.– Int. J. Thermal Sci., vol.48, pp.1108-1115. https://doi.org/10.1016/j.ijthermalsci.2008.11.012.

[8] Kumar R., Singh D.K. and Chander S. (2023): *Experimental study on flow condensation pressure drop of R123-MWCNTs nanorefrigerant*.– Int. J. Refrig., vol.154, pp.243–257. https://doi.org/10.1016/j.ijrefrig.2023.07.011

[9] Jiang W., Ding G., Peng H., Gao Y. and Wang K. (2009): *Experimental and model research on nanorefrigerant thermal conductivity*.– HVAC&R Research, vol.15, No.3, pp.651-669. https://doi.org/10.1080/10789669.2009.10390855.

[10] Ahmadpour M.M. and Akhavan-Behabadi M.A. (2019): *Experimental investigation of heat transfer during flow condensation of HC-R600a based nano-refrigerant inside a horizontal U-shaped tube*.– Int. J. Thermal Sci., vol.146, 106110. https://doi.org/10.1016/j.ijthermalsci.2019.106110.

[11] Eshgarf H. and Afrand M. (2016): *An experimental study on rheological behavior of non-Newtonian hybrid nano-coolant for application in cooling and heating systems*.– Exp. Therm. Fluid Sci., vol.76, pp.221-227. https://doi.org/10.1016/j.expthermflusci.2016.03.015.

[12] Sharma A.K., Tiwari A.K. and Dixit A.R. (2016): *Rheological behaviour of nanofluids: A review*.– Renew. Sustain. Energy Rev., vol.53, pp.779-791. http://dx.doi.org/10.1016/j.rser.2015.09.033.

[13] Mahbubul I.M., Khaleduzzaman S.S., Saidur R. and Amalina M.A. (2014): *Rheological behavior of Al2O3/R141b nanorefrigerant*.– Int. J. Heat Mass Transfer, vol.73, pp.118-123. http://dx.doi.org/10.1016/j.ijheatmasstransfer.2014.01.073.

[14] Raju R.S., Reddy B.M. and Reddy G.J. (2017): *Finite element solutions of free convective Casson fluid flow past a vertically inclined plate submitted in magnetic field in presence of heat and mass transfer*.– Int. J. for Comp. Methods in Engineering Science and Mechanics, vol.18, No.4-5, pp.250-265. https://doi.org/10.1080/15502287.2017.1339139.

[15] Reddy G.J., Raju R.S. and Rao J.A. (2018): *Influence of viscous dissipation on unsteady MHD natural convective flow of Casson fluid over an oscillating vertical plate via FEM*.– Ain Shams Eng. J., vol.9, No.4, pp.1907-1915. https://doi.org/10.1016/j.asej.2016.10.012.

[16] Prameela M., Gangadhar K. and Reddy G.J. (2022): *MHD free convective non-Newtonian Casson fluid flow over an oscillating vertical plate*.– Partial Differential Equations in Applied Mathematics, vol.5, 100366. https://doi.org/10.1016/j.padiff.2022.100366.

[17] Srividya K., Shamshuddin M.D., Salawu S.O. and Ram M.S. (2025): *Thermal radiative and viscous dissipative of gravity-driven magneto-Casson nanofluid in an isothermal stretching sheet*.– Int. J. Model. Simul., pp.1-17. https://doi.org/10.1080/02286203.2025.2475433.

[18] Shamshuddin M.D., Panda S., Salawu S.O., Mishra S.R. and Patil V.S. (2025): *Analysis of Casson ternary nanofluid integration under various thermal physical impacts with Cattaneo-Christov model: Exploring magnified heat transfer in stretchy surface*.– Int. J. of Hydrogen Energy, vol.101, pp.450-460. https://doi.org/10.1016/j.ijhydene.2024.12.426.

[19] Salawu S.O., Shamshuddin M.D., Mizan M.R.B. and Bari S. (2024): *Mathematical and Buongiorno nanofluid modelling to predict the thermal and solutal performance of magneto-bioconvective Casson nanofluid flowing in a rotatory disk*.– Phys. Scr., vol.99, No.12, 125239. DOI:10.1088/1402-4896/ad8e1a.

[20] Kasaeian A., Daneshazarian R., Mahian O., Kolsi L., Chamkha A.J., Wongwises S. and Pop I. (2017): *Nanofluid flow and heat transfer in porous media: A review of the latest developments*.– Int. J. Heat and Mass Transfer, vol.107, pp.778-791. https://doi.org/10.1016/j.ijheatmasstransfer.2016.11.074.

[21] Khanafer K. and Vafai K. (2019): *Applications of nanofluids in porous medium: A critical review*.– J. Therm. Anal. Calorim., vol.135, pp.1479-1492. https://doi.org/10.1007/s10973-018-7565-4.

[22] Menni Y., Chamkha A.J. and Azzi A. (2019): *Nanofluid transport in porous media: A review*.– Special Topics and Reviews in Porous Media: An International Journal, vol.10, No.1, pp.49-64. DOI:10.1615/SpecialTopicsRevPorousMedia.2018027168.

[23] Khalaf A.F., Basem A., Hussein H.Q., Jasim A.K., Hammoodi K.A., Al-Tajer A.M., Omer I. and Flayyih M.A. (2022): *Improvement of heat transfer by using porous media, nanofluid, and fins: A review*.– Int. J. Heat Technol., vol.40, No.2, pp.497-521. https://doi.org/10.18280/ijht.400218.

[24] Nandeppanavar M.M., Vaishali S., Kemparaju M.C. and Raveendra N. (2020): *Theoretical analysis of thermal characteristics of casson nano fluid flow past an exponential stretching sheet in Darcy porous media*.– Case Stud. Therm. Eng., vol.21, 100717. https://doi.org/10.1016/j.csite.2020.100717.

[25] Abo-Dahab S.M., Abdelhafez M.A., Mebarek-Oudina F. and Bilal S.M. (2021): *MHD Casson nanofluid flow over nonlinearly heated porous medium in presence of extending surface effect with suction/injection*.– Ind. J. Phys., vol.95, No.12, pp.2703-2717. https://doi.org/10.1007/s12648-020-01923-z.

[26] Sharanayya and Biradar S. (2023): *Magnetized dissipative Casson nanofluid flow over a stretching sheet with heat source/sink and soret effect under porous medium*.– J. Bionanosci., vol.13, No.4, pp.2103-2121. https://doi.org/10.1007/s12668-023-01184-0.

[27] Manthramurthy P. and Vempati S.R. (2025): *Significance of multiple slips and thermal radiation on heat and mass transfer in MHD Casson nanofluid flow over an exponentially stretching porous sheet with non-uniform heat source and sink*.– Multiscale Multidiscip. Model. Exp. Des., vol.8, No.3, pp.1-18. https://doi.org/10.1007/s41939-025-00743-0.

[28] Kumar V., Ram P. and Sharma K. (2025): *Inclined magnetized convective dissipation of radiative Casson nanofluid in porous medium with Soret effect*.– Eur. Phys. J. Spec. Top., pp.1-17. https://doi.org/10.1140/epjs/s11734-024-01439-1.

[29] Hafez N.M. and Abd-Alla A.M. (2025): *Thermally MHD peristaltic flow of a Casson fluid-particle suspension with the impacts of electroosmosis and mass transmission in a porous medium*.– J. Therm. Anal. Calorim., vol.150, pp.2249-2272. https://doi.org/10.1007/s10973-024-13710-7.

[30] Govindaraj N., Iyyappan G., Barman T., Shukla P. and Singh A.K. (2025): *A numerical study of Casson nanofluid flow embedded in a riga plate with irregular boundaries*.– J. Porous Media, vol.28, No.5, pp.89-106. DOI:10.1615/JPorMedia.2024051989.

[31] Manideep P., Raju R.S., Rao T.S.N. and Reddy G.J. (2018): *Unsteady MHD free convection flow of Casson fluid over an inclined vertical plate embedded in a porous media*.– In AIP Conference Proceedings, vol.1953, No.1, p.140038. https://doi.org/10.1063/1.5033213.

[32] Kumar M.A., Pothanna N. and Reddy G.J. (2025): *Analyzing the heat and mass transfer behavior in a 2-D forchheimer porous medium on MHD Casson fluid flow over an inclined non-linear surface with viscous dissipation, chemical reaction, and Soret–Dufour parameters*.– Multiscale Multidiscip. Model. Exp. Des., vol.8, No.3, p.176. https://doi.org/10.1007/s41939-025-00767-6.

[33] Panda S., Shamshuddin M.D., Pattnaik P.K., Mishra S.R., Shah Z., Alshehri M.H. and Vrinceanu N. (2024): *Ferromagnetic effect on Casson nanofluid flow and transport phenomena across a bi-directional Riga sensor device: Darcy-Forchheimer model*.– Nanotechnol. Rev., vol.13, No.1, 20240021. https://doi.org/10.1515/ntrev-2024-0021.

[34] Chandrasekar M., Suresh S. and Senthilkumar T. (2012): *Mechanisms proposed through experimental investigations on thermophysical properties and forced convective heat transfer characteristics of various nanofluids-A review*.– Renew. Sustain. Energy Rev., vol.16, No.6, pp.3917-3938. https://doi.org/10.1016/j.rser.2012.03.013

[35] Telles R.S. and Trevisan O.V. (1993): *Dispersion in heat and mass transfer natural convection along vertical boundaries in porous media*.– Int. J. Heat and Mass Transfer, vol.36, No.5, pp.1357-1365. https://doi.org/10.1016/S0017-9310(05)80103-6.

[36] Yang C. and Nakayama A. (2010): *Synthesis of tortuosity and dispersion in effective thermal conductivity of porous media*.– Int. J. Heat and Mass Transfer, vol.53, No.15-16, pp.3222–3230. https://doi.org/10.1016/j.ijheatmasstransfer.2010.03.004.

[37] Fried J.J. and Combarnous M.A. (1971): *Dispersion in porous media*.– Adv. Hydrosci., vol.7, pp.169-282. https://doi.org/10.1016/B978-0-12-021807-3.50008-4.

[38] Kvernvold O. and Tyvand P.A. (1980): *Dispersion effect on thermal convection in porous media*.– J. Fluid Mech., vol.99, No.4, pp.673–686. https://doi.org/10.1017/S0022112080000821.

[39] Hsu C.T. and Cheng P. (1980): *Thermal dispersion in a porous medium*.– Int. J. Heat Mass Transfer, vol.33, No.8, pp.1587-1597. https://doi.org/10.1016/0017-9310(90)90015-M.

[40] Lai C. and Kulacki F.A. (1989): *Thermal dispersion effects on non-Darcy convection over horizontal surfaces in saturated porous media*.– Int. J. Heat Mass Transfer, vol.32, No.5, pp.971-976. https://doi.org/10.1016/0017-9310(89)90246-9.

[41] Cheng P., Ali C.L. and Verma A.K. (1981): *An experimental study of non-Darcian effects in free convection in a saturated porous medium*.– Lett. Heat Mass Transfer, vol.8, No.4, pp.261-265. https://doi.org/10.1016/0094-4548(81)90040-0.

[42] Plumb O.A. and Huenefeld J.C. (1981): *Non-Darcy natural convection from heated surfaces in saturated porous media*.– Int. J. Heat Mass Transfer, vol.24, No.4, pp.765-768. https://doi.org/10.1016/0017-9310(81)90020-X.

[43] Cheng P. (1981): *Thermal dispersion effects in non-Darcian convective flows in a saturated porous medium*.– Lett. Heat Mass Transfer, vol.8, No.4, pp.267-270. https://doi.org/10.1016/0094-4548(81)90041-2.

[44] Hong J.T. and Tien C.L. (1987): *Analysis of thermal dispersion effect on vertical plate natural convection in porous media*.– Int. J. Heat and Mass Transfer, vol.30, No.1, pp.143-150. https://doi.org/10.1016/0017-9310(87)90067-6

[45] Özgümüş T., Mobedi M., Özkol Ü. and Nakayama A. (2013): *Thermal dispersion in porous media-A review on the experimental studies for packed beds*.– Appl. Mech. Rev., vol.65, No.3, 031001. https://doi.org/10.1115/1.4024351

[46] Saada M.A., Chikh S. and Campo A. (2006): *Analysis of hydrodynamic and thermal dispersion in porous media by means of a local approach*.– Heat and mass transfer, vol.42, No.11, pp.995-1006. https://doi.org/10.1007/s00231-005-0061-y.

[47] Venkata Ramudu A.C., Anantha Kumar K., Sugunamma V. and Sandeep N. (2020): *Heat and mass transfer in MHD Casson nanofluid flow past a stretching sheet with thermophoresis and Brownian motion*.– Heat Transf., vol.49, No.8, pp.5020–5037. https://doi.org/10.1002/htj.21865.

[48] Nakamura M. and Sawada T. (1988): *Numerical study on the flow of a non-Newtonian fluid through an axisymmetric stenosis*.– J. Biomech. Eng., vol.110, No.2, pp.137-143. https://doi.org/10.1115/1.3108418.

[49] Nield D.A. and Kuznetsov A.V. (2011): *The Cheng-Minkowycz problem for the double-diffusive natural convective boundary layer flow in a porous medium saturated by a nanofluid*.– Int. J. Heat and Mass Transfer, vol.54, pp.374-378. https://doi.org/10.1016/j.ijheatmasstransfer.2010.09.034.

[50] Bouaziz A.M. and Hanini S. (2016): *Double dispersion for double diffusive boundary layer in non-Darcy saturated porous medium filled by a nanofluid*.– J. Mech., vol.32, No.4, pp.441-451. https://doi.org/10.1017/jmech.2016.18.

Received: April 19, 2025

Revised: February 24, 2026